Construction of a Novel Redox Protein by Rational Design: Conversion of a Disulfide Bridge into a Mononuclear Iron−Sulfur Center†

David E. Benson,‡ Michael S. Wisz,‡ Wentian Liu, and Homme W. Hellinga*

Department of Biochemistry, Box 3711, Duke University Medical Center, Durham, North Carolina 27710

Received March 16, 1998; Revised Manuscript Received April 8, 1998

ABSTRACT: A mononuclear iron-sulfur center, capable of reversible electron transfer, has been introduced into thioredoxin, a protein devoid of such sites, using an automated, structure-based design algorithm. One of the sites predicted by the Dezymer computer program to introduce a tetrahedral tetrathiolate iron center included the intrinsic Cys32−Cys35 disulfide of wild-type thioredoxin and two additional mutants, Trp28Cys and Ile75Cys, thereby converting a disulfide into a metal-based redox center. This designed protein forms a 1:1 monomeric complex with Fe^{III}, whose electronic absorption and EPR spectra closely resemble those of the rubredoxins, as intended. Co^{II} spectra provided further confirmation of tetrahedral tetrathiolate metal coordination. The designed protein is capable of undergoing successive cycles of oxidation and reduction. The computer-generated design only took into account the geometry of the primary coordination shell around the metal. We have therefore demonstrated that simple geometrical considerations can be sufficient to reproduce the dominant electronic structure and reactivity of a simple metal-based redox center.

Rational design can be used as a tool to investigate general principles in the relationship between protein structure and function (*1*−*3*). One approach starts with designs based on the simplest, or minimalist, model of a system and iteratively introduces additional levels of complexity on the basis of results obtained from the experimental implementation of the previous design cycle (*4*). This methodology aims to uncover a minimally sufficient set of components that dominate the formation of the desired structure or function. Metalloprotein centers are ideally suited to the design of protein function in this manner (*5*−*7*), because the interactions that determine the interplay between the intrinsic properties of the metal center itself and the surrounding protein matrix, thereby controlling structure and reactivity (*8*), can be classified into a clear hierarchy. The properties of a metal center are dominated by the composition, number, and geometry of ligands in the primary coordination sphere (*9*). The next most dominant factors are hydrogen bonding and steric interactions between the primary coordination sphere and its immediate surroundings (secondary coordination shell). The final level of modulation arises from interactions dispersed throughout the protein which introduce long-range electrostatic factors due to the distribution of charged residues and proximity to the solvent (*10*). Thus, an iterative design strategy can be devised where increasingly long-range interactions are introduced in a design series that starts with the construction of just a primary coordination sphere.

Here we present the construction of a metal-based redox center in *Escherichia coli* thioredoxin, a protein devoid of such sites (*11*). The design was based on a mononuclear iron-sulfur center. Such sites are the simplest members of the iron-sulfur clusters family which constitute an important class of prosthetic groups that participate in a wide variety of biological reactions (*12*). The sites in typical members of mononuclear iron-sulfur proteins, such as rubredoxins and desulforedoxins (*13*), are formed through tetrahedral coordination by four cysteines and usually function in electron transport pathways. Two of the cysteines in one of the predicted sites from this study were contributed by the disulfide bridge of the original thioredoxin active site (*14*). This design therefore involves the conversion of a disulfide into a metal-based redox center. The design was generated by an automated design procedure, Dezymer (*15*), which takes into account only the geometry of the primary coordination sphere and its approximate steric compatibility with the surrounding protein matrix (*16*−*19*). We demonstrate that such simple models are sufficiently powerful to reproduce the major features of the electronic structure and reactivity of a mononuclear iron-sulfur redox center.

MATERIALS AND METHODS

Solutions were prepared with water with 18 MΩ resistance. All solutions, unless containing EDTA,[1] were extracted with dithizone/chloroform mixtures (*20*) to further remove metals from solution.

† This work was supported by Grant R29GM49871 from the National Institutes of Health to H.W.H. M.S.W. acknowledges support from a training grant from the National Institutes of Health (5T32-GM-08487-04).

* To whom correspondence should be addressed. Telephone: (919) 681-5885. Fax: (919) 684-8885. E-mail: hellinga@linnaeus.biochem.duke.edu.

‡ Both authors contributed equally to this work.

[1] Abbreviations: βME, β-mercaptoethanol; DTNB, 5,5′-dithiobis-(2-nitrobenzoic acid); DTT, 1,4-dithiothreitol; EDTA, ethylenediaminetetraacetic acid; EPR, electron paramagnetic resonance; IPTG, isopropyl β-D-thiogalactopyranoside; LMCT, ligand-to-metal charge transfer; MBP, maltose binding protein; Polymin-P, polyethylenimine; SDS, sodium dodecyl sulfate; TCEP, tris(2-carboxyethyl)phosphine chloride; TrisHCl, tris(hydroxymethyl)aminomethane hydrochloride; Trx[Rd], mutant thioredoxin with designed Cys_4 rubredoxin-like metal center.

S0006-2960(98)00583-2 CCC: $15.00
Published on Web 04/30/1998

Mutagenesis. Thioredoxin mutants were constructed by oligonucleotide-directed mutagenesis (*21*) in a *trxA* gene that contains two additional mutations: an Asp2Ala mutation for removing an adventitious surface metal binding site (*22*, *23*) and an Asp26Leu mutation for increasing protein stability (*24*). The Trp28Cys and Ile75Cys mutants were made using the oligonucleotides 5′-GCA CCA CTC TGC GCA GAA ATC GAC GAG GAT CGC-3′ and 5′-CAG CAG AGT CGG GCA ACC ACG GAT GCC-3′, respectively (mutant codons underlined). The *trxA* gene is expressed as a fusion protein at the C terminus of maltose binding protein (MBP) using a derivative of the expression vector pMAL-c2 (*25*; New England Biolabs) in which a flexible peptide linker containing a unique thrombin cleavage site (Ile-Glu-Gly-Arg-Ile-Ser-Glu-Phe-Gly-Ser-Leu-Val-Pro-Arg-Gly-Ser-Gly-Gly-Ser-Gly-Gly-Ser) has been placed between the MBP and the Trx domain. The resulting fusion protein is readily purified in a single step on an amylose affinity column.

Protein Production and Purification. Fusion proteins were prepared as follows. *E. coli* XL1-Blue cells were transformed with pMAL-c2 containing the mutated *trxA* gene cloned into a unique *Bam*HI restriction site, and selected on 2xYT ampicillin (100 μg/mL) plates. Cultures of 120 mL (2xYT and 25 μg/mL ampicillin) were inoculated with a single transformed colony and grown at 37 °C overnight. This starter culture was used to inoculate 6 L of 2xYT and 0.2% glucose, which was grown at 37 °C to an A_{600} of 0.6. IPTG (1 mM final concentration) was added to induce protein overexpression, and the culture was grown for a further 4 h. Cells were harvested by centrifugation, resuspended in ice-cold TSE buffer [20 mM Tris-HCl (pH 7.5), 200 mM NaCl, and 10 mM EDTA], and stored at −80 °C. Resuspended cells were lysed in a French press; a cleared lysate was prepared by centrifugation, and nucleic acids were precipitated with 0.5% (w/v) polymin-P (Sigma) at pH 8.0 and removed by a second centrifugation. The supernatant was loaded on an amylose affinity column (New England Biolabs), pre-equilibrated with 2 volumes of TSE. The column was then washed with 2 volumes of metal-free TS [20 mM Tris-HCl (pH 7.5) and 200 mM NaCl] and eluted with metal-free TSM (TS and 10 mM maltose). The resulting protein was judged to be pure by SDS−polyacrylamide electrophoresis.

Protein Determinations. The extinction coefficient at 280 nm (ϵ_{280}) was determined to be 76.7 mM^{-1} cm^{-1} for the apo-Trx[Rd] fusion protein by the Edelhoch method (*27*) and was used to quantitate protein in the absence of a metal chromophore. The protein concentration of metal-containing samples was determined colorimetrically (*28*), using standard curves calibrated with apo-Trx[Rd].

In Vitro Reconstitution with Metal. To prepare reduced, metal-free apoprotein, the affinity-purified protein was concentrated by ultrafiltration using an Amicon YM-10 membrane and incubated overnight at 4 °C in 50 mM EDTA, 50 mM DTT, and 2 mM *o*-phenanthroline. Dioxygen was removed by purging with argon in a Teflon-sealed vial. Chelators and reductants were removed by gel filtration in an anaerobic glovebox using a P-6 matrix (Bio-Rad), eluted with argon-purged TS. Free thiols were determined spectrophotometrically using DTNB (ϵ_{412} = 13.7 mM^{-1} cm^{-1}; *26*). In the anaerobic box, dioxygen contamination was low enough to oxidize only 0.1 free thiol (out of 4.0 free thiols) of apo-Trx[Rd] stored over 4 days at room temperature (half-life of apo-Trx[Rd] oxidation is around 45 min in air).

Metal complexes were prepared anaerobically in a glovebox or on a Schlenk line by direct addition of metal to apo-Trx[Rd] in TS buffer. A binding isotherm taking into account all species was used to fit the observed absorbance changes:

$$A = A_o + (A_{max} - A_o) \times \frac{([P]_t + [M]_t + K_d) - \sqrt{([P]_t + [M]_t + K_d)^2 - 4[P]_t[M]_t}}{2[P]_t} \quad (1)$$

where A_o, A, and A_{max} are the absorbances at 670 nm in the absence, in the presence, and at saturation of metal, respectively, $[P]_t$ is the total concentration of Trx[Rd], $[M]_t$ is the total concentration of metal at each titration point, and K_d is the dissociation constant for the metalloprotein complex.

Iron Determinations. The concentrations of total iron in samples were determined colorimetrically (*29*). Fe−Trx[Rd] was heat denatured and any Fe^{III} reduced with hydroxylamine and reacted with *o*-phenanthroline to form the colored complex (ϵ_{512} = 10.9 mM^{-1} cm^{-1}). To obtain iron incorporation ratios, protein concentrations were determined using the Bradford assay (see above).

Electronic Absorbance Spectroscopy. All electronic absorbance spectra were recorded at room temperature on a Hitachi U-2000 spectrophotometer. Anaerobic spectra were recorded in Teflon-sealed cuvettes (Hellma), which were deoxygenated either by loading samples inside an anaerobic box or by purging with argon on a dual-manifold Schlenk line.

EPR Spectroscopy. All Fe−Trx[Rd] samples were air-oxidized, placed in standard inner diameter quartz EPR tubes (quantitative grade, Wilmad), and frozen in liquid nitrogen and their spectra recorded at 100 ± 1 K (liquid nitrogen cryostat) on a X-band EPR spectrometer (JEOL USA) with a TE_{102} cavity (9.180 GHz, 1 mW power, 1 mT modulation, 0.01 s time constant). Relative signal intensity was quantitated from the double-integrated area of each EPR spectrum (*30*) using Kaleidagraph (Abelbeck Software).

RESULTS

Design of the Tetrahedral Cys_4 Site in Thioredoxin. The Dezymer automated design algorithm (*15*) systematically examines a protein of known structure to identify locations where appropriate side chain rotamers can be placed to introduce a coordination sphere of predetermined geometry while maintaining steric compatibility with the protein fold. The protein backbone is kept fixed throughout the search. The algorithm uses a simple description of molecular interactions in which the primary coordination sphere of the metal is specified in purely geometrical terms (bond lengths, angles, and torsional relationships) and all other, nonbonded interactions by a hard-sphere model. At the conclusion of the search, the sites are rank-ordered according to a score $U(p)$ that reflects the least-squares deviation from the ideal tetrahedral geometry.

The predictions were calculated using an idealized tetrahedral geometry around the iron center (*31*), 2.3 Å for the

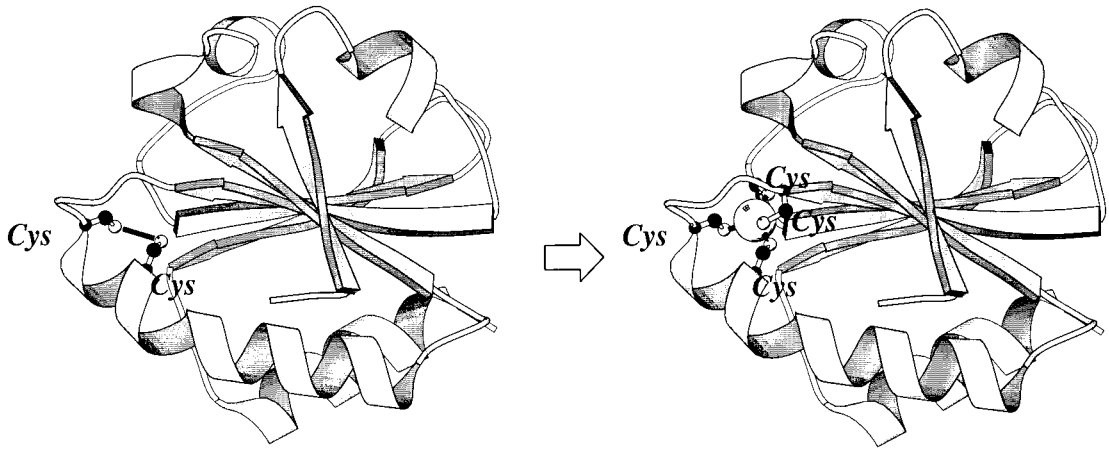

FIGURE 1: Conversion of the disulfide bridge (C32−C35) of thioredoxin into an FeS_4 center (Trx[Rd]) by the introduction of two additional cysteines (W28C and I75C). This figure was generated with Molscript (*50*).

S_γ−Fe bond lengths (*32*), and a small cysteine rotamer library consisting of three members that represent the preferred g^+, g^-, and t conformers (*33*). Approximately 150 potential solutions were identified in the high-resolution X-ray structure of the oxidized form of *E. coli* thioredoxin (*23*) and rank-ordered according to their $U(p)$ scores. The second-highest ranked site used Cys32 and Cys35, which form the disulfide bridge in the active site of wild-type thioredoxin, as two of the ligands and predicted that the introduction of two additional mutations, Trp28Cys and Ile75Cys, should complete a tetrahedral Cys_4 site (Figure 1). Visual inspection of this model indicated that no additional mutations were necessary to alleviate adverse steric interactions, although the loss in side chain volume introduced by the two mutations means that the core of the loop region in which the original disulfide is located becomes slightly underpacked around the designed site. Because of its reasonable geometry and the possibility of converting a disulfide bridge into a mononuclear iron-sulfur center, we chose to construct this site which we have named Trx[Rd].

Preparation of the Designed Protein. The Trp28Cys/Ile75Cys double mutant, Trx[Rd], is most easily expressed in large quantities (typically ∼150 mg/L of cell culture) and purified by single-step affinity chromatography as a C-terminal fusion with maltose binding protein (MBP). Since MBP does not contain any metal binding sites, the spectroscopic properties of the designed metal center could be studied in the fusion construct. Determination of the stability of Trx[Rd] required proteolytic cleavage and further purification to remove the MBP moiety (*19*).

In Vitro Formation of the Iron Complex. The iron complex was prepared by direct titration with iron using a well-established procedure for the reconstitution of iron-sulfur proteins (*34*−*37*) in which $(NH_4)_2Fe(SO_4)_2$ is added anaerobically to purified apo-Trx[Rd] in the presence of excess βME (50 mM) in a glovebox or Schlenk line. One equivalent of Fe^{II} added to 100 μM apo-Trx[Rd] formed a faintly pink complex which immediately turned red upon exposure to air (Figure 2A). Addition of 100 μM $(NH_4)_2$-$Fe(SO_4)_2$ to reconstitution solutions in which the apo-Trx[Rd] either was omitted or had been replaced with wild-type thioredoxin did not result in the formation of such colored complexes, either anaerobically or upon air oxidation (Figure 2B). The red Fe^{III}−Trx[Rd] complex could be stably separated from unbound iron by gel filtration (PD-10, Pharmacia), eluting with 50 mM borate (pH 10.0), 200 mM NaCl, and 50 mM βME.

In Vivo Formation of the Iron Complex. It was found that the red complex can also form in vivo and could be purified directly from cells that overexpress Trx[Rd] by omitting βME and chelating reagents from the purification buffers. The wild-type thioredoxin fusion protein purified under similar conditions did not yield a colored protein. The electronic absorption spectra of the in vivo-formed Fe−Trx[Rd] can be superimposed on those of the in vitro-formed material, after metal concentration is taken into account.

Stoichiometry and Stability of the Iron Complex. Formation of the red complex could be followed in a titration experiment in which $(NH_4)_2Fe(SO_4)_2$ was added stepwise to 50 μM apo-Trx[Rd] in reconstitution buffer. After each addition, the solution was oxidized by exposure to air and the absorbance at 345 nm recorded. The resulting titration shows that the red complex is saturated when 1 equiv of Fe^{III} has been added (Figure 2C, filled circles). Furthermore, this complex could be bleached by the addition of 1 equiv of zinc (Figure 2C, open circles). The stoichiometries of stable, purified red complexes were also determined using colorimetric assays for protein and iron. Material purified by gel filtration from an in vitro reconstitution was found to contain 0.9 ± 0.2 equiv of iron per protein. In vivo-expressed Fe−Trx[Rd] showed 20% iron incorporation.

To establish the oligomeric state of the red protein, Fe−Trx[Rd] was chromatographed on a S200 (Pharmacia) gel filtration column, capable of distinguishing between monomeric and higher-order assemblies. Fe−Trx[Rd] was found to coelute with monomeric apo-Trx[Rd] at around 70 kDa (data not shown).

A binding constant for Fe^{III} could be estimated from the direct titration series (Figure 2C), fitting the observations to eq 1, and was found to be 0.7 μM. This is an upper limit for the K_d, however, since the binding is near-stoichiometric,[2] and the iron is added in the presence of excess βME which also binds iron, so that the true concentration of free iron is unknown and underestimated.

[2] Under this condition, fits to eq 1 become underdetermined at low K_d values.

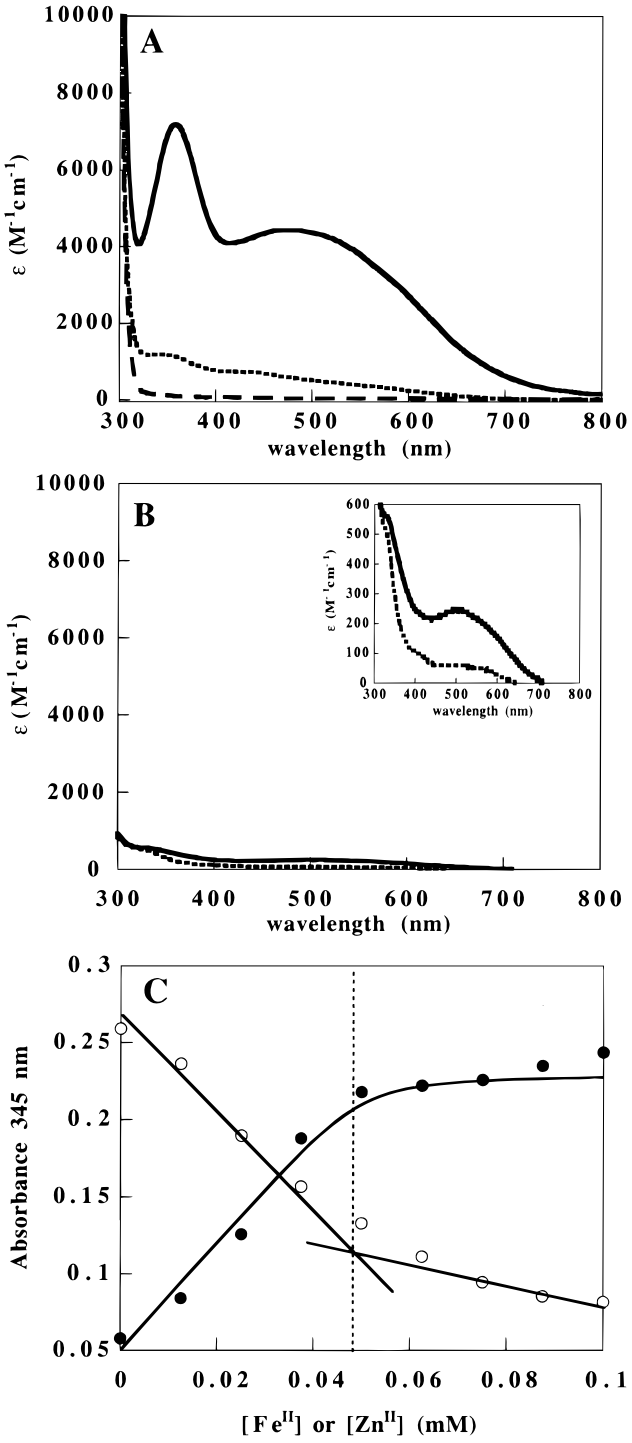

FIGURE 2: Electronic absorption spectra of iron complexes. (A) Addition of iron to apo-Trx[Rd] [100 μM protein, 50 mM βME, 200 mM NaCl, and 20 mM Tris-HCl (pH 7.5)]: apoprotein only (dashed line), anaerobic addition of 1 equiv (100 μM) of $(NH_4)_2$-$Fe(SO_4)_2$ (dotted line), and anaerobic addition followed by air oxidation (solid line). (B) Same experimental conditions, but replacing Trx[Rd] with wild-type thioredoxin (fused to MBP): 100 μM Fe^{II} (dotted line) followed by air oxidation (solid line). The inset is the rescaled spectrum. (C) Stoichiometry of the iron complex determined by direct spectrophotometric titration measured at 345 nm: (●) titration of apo-Trx[Rd] with Fe^{II} (50 μM protein), followed by air oxidation to obtain the Fe^{III} complex; and (○) addition of Zn^{II} to the saturated Fe^{III}−Trx[Rd] complex.

EPR Spectroscopy. X-band EPR spectra of purified Fe^{III}−Trx[Rd] complexes prepared in vitro or in vivo were recorded at 100 K. A single broad rhombic resonance was seen at g = 4.290 (Figure 3A), which was distinct from the resonance observed for Fe^{III} free in solution (~50 G upfield, data not shown). Apo-Trx[Rd] showed no such resonance. The double-integrated area of the g = 4.290 resonance scales linearly both with the amount of metal incorporation and with the intensity of the red chromophore (Figure 3B). Electronic absorption spectra were recorded before and after freezing samples in liquid nitrogen and showed a less than 10% decrease in absorbance at 350 nm after thawing.

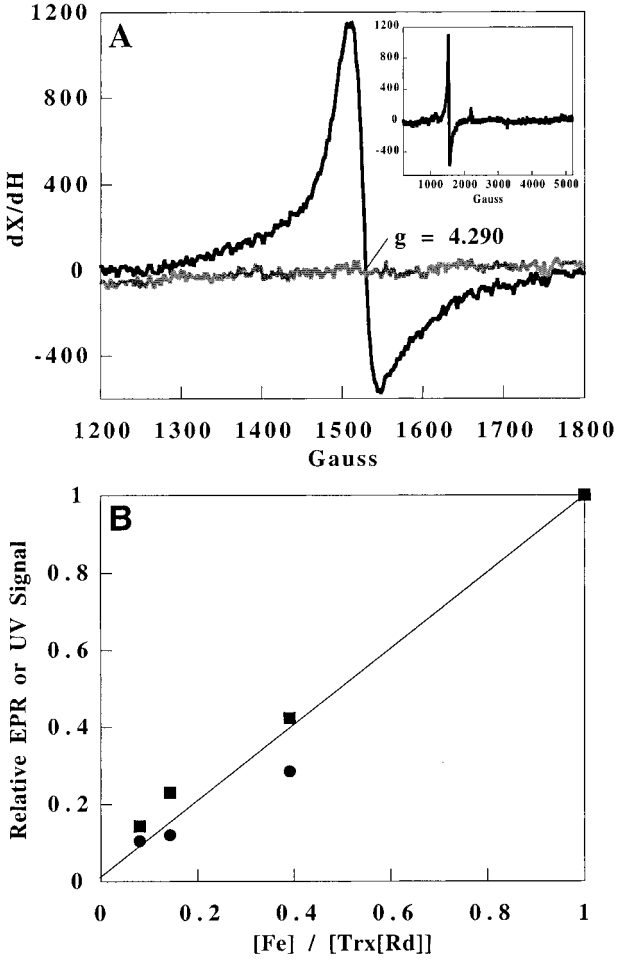

FIGURE 3: 100 K X-band EPR spectra of Fe^{III}−Trx[Rd]. (A) Spectra of 100 μM 1:1 in vitro-reconstituted Fe^{III}−Trx[Rd] (black line) and 100 μM apo-Trx[Rd] (gray line). The inset is the full spectrum of 1:1 reconstituted Fe−Trx[Rd], demonstrating the lack of any other significant resonances. (B) Correlation of EPR signal intensities with protein-bound Fe^{III} concentrations. Double-integrated area of EPR spectra (■) and absorbance of the red chromophore at 350 nm (●), normalized to Trx[Rd] concentrations, plotted against the ratio of Fe^{III} to protein concentration from three different preparations of in vivo-expressed and in vitro-incorporated metalloprotein.

Cobalt(II) Complex. To further characterize the coordination geometry, $CoCl_2$ was titrated into apo-Trx[Rd] under anaerobic conditions. The final spectrum (Figure 4) showed d−d transitions consistent with the energies (600−700 nm) and intensities (300−350 M^{-1} cm^{-1}) expected for tetrahedral Cys_4 Co^{II} complexes and transitions in the 350−450 nm region, consistent with four-thiolate ligation (*38*). This is also observed in Co^{II}-substituted rubredoxins (*39*, *40*), confirming the recapitulation of the geometry of the natural centers in this designed protein. A binding constant for Co^{II} could be deduced by measuring the absorbance at 670 nm as a function of added metal, and it was found to have a K_d

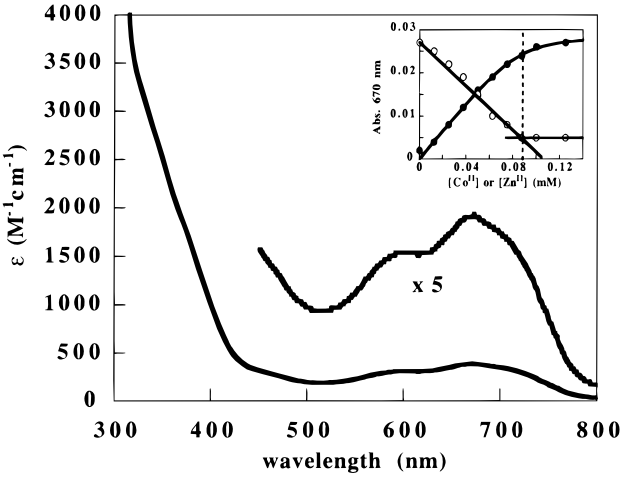

FIGURE 4: Electronic absorption spectra of the Co^{II} complex [anaerobic, 90 μM protein, 200 mM NaCl, 20 mM Tris-HCl (pH 7.5), and 100 μM $CoCl_2$]. The inset shows titration of $CoCl_2$ (●) and competitive titration of the Co^{II} complex with $ZnCl_2$ (○).

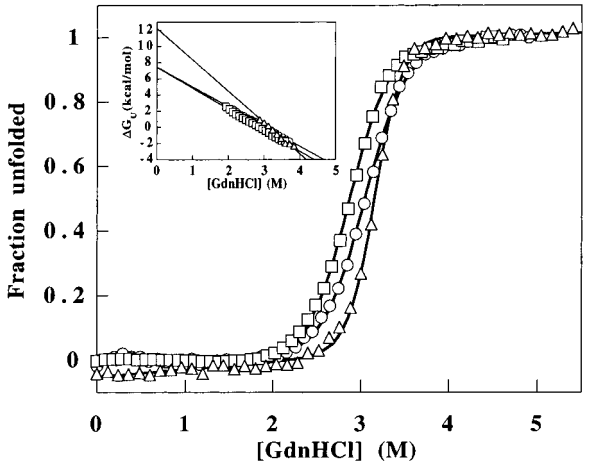

FIGURE 5: Stability of the designed protein. The free energy of unfolding (ΔG_U) was determined by chemical denaturation with guanidinium chloride (GdnHCl). The inset is the linear free energy extrapolation to 0 M denaturant: (△) C32S/C35S double mutant of wild-type thioredoxin that mimics the reduced form (ΔG_U = 12.2 ± 0.2 kcal mol^{-1}), (□) Trx[Rd] in the presence of 1 equiv of Zn^{II} (ΔG_U = 7.4 ± 0.1 kcal mol^{-1}), and (○) apo-Trx[Rd] (ΔG_U = 7.4 ± 0.1 kcal mol^{-1}).

of less than 5 μM (inset of Figure 4). Finally, the Co^{II} complex could be displaced by titration with 1 equiv of $ZnCl_2$.

Protein Stability. Stability measurements were performed on purified Trx[Rd] prepared from the fusion protein by proteolytic cleavage as described elsewhere (*19*). Free energies of unfolding were determined by chemical denaturation in the presence and absence of zinc[3] and fit to a two-state model (*41*). Although the Trx[Rd] is destabilized relative to wild-type thioredoxin (Figure 5), it still folds. Zinc had little or no effect on stability, indicating that the metal binds equally well to the folded and unfolded states (*19*), presumably because the coordinating residues are close to each other in both states.

Redox Activity. To qualitatively establish whether Fe−Trx[Rd] is capable of acting as a redox center, reconstituted

[3] Zn^{II}, rather than Fe^{II}, was used to avoid complications due to metal-mediated oxidation of the cysteines in the unfolded state (this can occur even anaerobically).

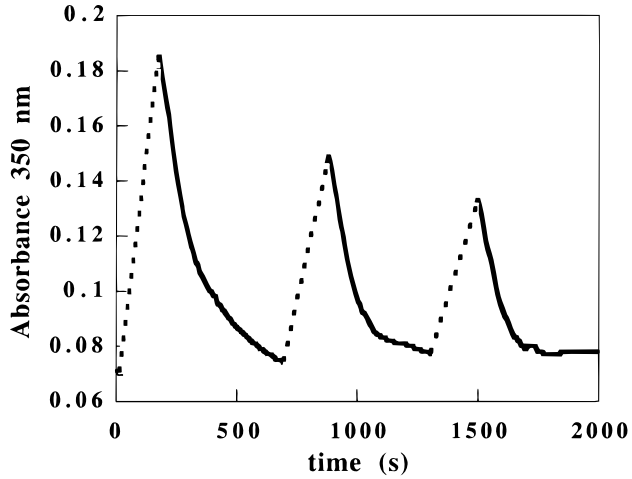

FIGURE 6: Redox cycling of 40 μM Fe−Trx[Rd] in the presence of 50 mM βME, 200 mM NaCl, and 20 mM Tris-HCl (pH 7.5). In repeated cycles, oxidative conditions were first established by aeration of the protein solution (dashed lines), followed by placement of the solution in an airtight cuvette and spectroscopic monitoring of reduction by βME (solid lines).

protein in 50 mM βME was subjected to successive cycles of oxidative and reductive conditions, monitoring the absorbance at 350 nm to follow the redox state of the metal. Oxidation of the metal center was achieved by aeration of the solution. Reductive conditions were re-established by closing the cuvette to exclude excess oxygen, thereby allowing the βME to reduce the metal. In this manner, several successive redox cycles could be observed (Figure 6).

DISCUSSION

The intent of the design was to construct a stable, monomeric protein that forms a tetrahedral, Cys_4 coordination complex with iron that is capable of repeated redox cycles and is an analogue of the natural mononuclear iron-sulfur proteins. Here we demonstrate that we have achieved this goal.

Structure of the Designed Metal Center. Iron forms a stable complex with Trx[Rd] (Figure 2A), which can be prepared either by in vitro reconstitution or by in vivo incorporation. This complex forms with a 1:1 Fe:protein stoichiometry, as demonstrated in vitro by direct spectrophotometric titration of the Fe^{III} complex ($K_d \leq 0.7$ μM; Figure 2), by bleaching of this complex by 1 equiv of zinc (Figure 2), and by determination of the amount of iron incorporated relative to protein in a complex purified from the in vitro reconstitution reaction by gel filtration. Furthermore, the intensity of the chromophore scaled linearly with the amount of in vivo-incorporated iron. The hydrodynamic behavior of the iron complex is identical to that of the monomeric apoprotein, indicating that there is no appreciable metal-mediated oligomerization. We therefore conclude that the designed protein forms a single iron site that is spectroscopically active and that does not form in the parent protein, as intended.

The electronic absorption spectrum of the red complex (Figure 2A) has broad absorbances tailing from the UV with peaks at ~360 and ~490 nm and a shoulder around 580 nm, similar to mononuclear FeS_4 metalloproteins (*42*−*45*) and a tetrathiolate synthetic model complex (*46*, *47*). The

electronic properties of Fe^{III}−Trx[Rd] most closely match those of the synthetic model and are similar to those of the rubredoxins, consistent with the formation of a mononuclear tetrahedral, tetrathiolate iron-sulfur coordination complex. This is further supported by the 100 K EPR spectrum (Figure 3A) which shows a single, broad, rhombic resonance at $g = 4.290$, distinguishing the site from polynuclear iron-sulfur centers. The intensity of this resonance scales linearly both with the amount of incorporated iron and with the intensities of the red chromophore (Figure 3B) and therefore is due to the same chromophore that gives rise to the red complex, and not to some other, adventitiously bound iron species. Finally, the tetrahedral, tetrathiolate geometry of the designed site is confirmed by the characteristic absorption spectrum of the Co^{II} complex (Figure 4). We therefore conclude that we have constructed a mononuclear iron-sulfur center with the intended geometry.

Reactivity. The Fe−Trx[Rd] complex is capable of undergoing several successive cycles of air oxidation and reduction by βME (Figure 6). The maximum absorbance of the oxidized form decayed in each successive cycle, presumably reflecting accumulative oxidative damage as is frequently observed in iron−sulfur centers upon air exposure (*34*, *36*). We have therefore qualitatively established that the designed protein has the intended reactivity and is capable of reversible electron transfer.

Conclusions. We have demonstrated that a redox-active mononuclear iron-sulfur center has been introduced into *E. coli* thioredoxin using a structure-based design approach. The automated design algorithm revealed that a geometrical accident of history allowed for the conversion of a pre-existing redox-active disulfide bridge into a tetrahedral Cys_4 mononuclear iron center by the introduction of two additional cysteines. Thus, one type of redox center was switched to another. This extends the range of metal centers introduced into this protein using the Dezymer program, including an Fe_4S_4 iron-sulfur cluster (*16*), an Fe-based superoxide dismutase (*18*), a family of Cys_2His_2 zinc centers (*19*), and a blue copper analogue (*17*). This demonstrates the robustness of the design approach and the remarkable capacity of a simple protein to "evolve" into a divergent family of metalloproteins.

The mononuclear iron-sulfur site was designed using a minimalist model in which only the geometry of the primary coordination and its approximate steric compatibility with the surrounding protein are taken into account, but lacks secondary shell interactions such as the hydrogen bonds to the coordinating thiols observed in the crystal structures of the natural sites (*31*). These results indicate that a correctly formed primary coordination sphere by itself is sufficient to reproduce the dominant features of structure and reactivity of mononuclear iron-sulfur metal centers. This is further emphasized by the lack of sequence or structural homology between this design and the native proteins. The spacing between the cysteines in the primary coordination sphere (Cys-X_3-Cys-X_2-Cys-X_{39}-Cys) bears no resemblance to the consensus spacings (*48*) observed in rubredoxins (Cys-X_2-Cys-X_n-Cys-X_2-Cys) or desulforedoxins (Cys-X_2-Cys-X_m-Cys-Cys). Likewise, neither the secondary nor tertiary environments show any similarities, since in the designed protein two of the cysteines are located within one turn of an α-helix (C32 and C35) and the other two (C28 and C75) are situated on adjacent β-strands, whereas the cysteines in the native proteins are positioned in β-hairpin loops.

Comparison of the detailed optical spectra reveals a number of differences, however, which must reflect variations in the protein environment. In particular, the electronic transitions of the Fe^{III}−Trx[Rd] complex are broader than those observed in native proteins. Since the majority of the contributions to the electronic absorption spectrum are thought to stem from LMCT bands involving the Sp^{σ} and Sp^{π} orbitals overlapping with the $Fe_{d_{xy}}$ and $Fe_{d_{xz,yz}}$ orbitals (*34*, *49*), the broad absorption bands may be due to microheterogeneity of the iron ligation sphere. This can be ascribed to increased flexibility of the designed site, which in turn can be attributed to a decrease in the local packing density around this site, consistent with the lowered stability of the designed protein. This design therefore represents the first step in an iterative design process in which additional levels of complexity can be introduced in subsequent design cycles to systematically test how changes in local packing interactions, hydrogen bonding to cysteines, and long-distance electrostatic interactions affect the electronic structure and reactivity of the center.

ACKNOWLEDGMENT

We thank Dr. Irwin Fridovich for the generous donation of the LabConco anaerobic box utilized in this work. We also thank E. J. Harbron, E. K. Warmouth, and Dr. M. D. E. Forbes, in the Chemistry Department of the University of North Carolina at Chapel Hill, for assistance in obtaining EPR spectra and V. J. Zhang for assistance with mutagenesis.

REFERENCES

1. Bryson, J. W., Betz, S. F., Lu, H. S., Suich, D. J., Zhou, H. X., O'Neil, K. T., and DeGrado, W. F. (1995) *Science 270*, 935−941.
2. Dahiyat, B. I., and Mayo, S. L. (1997) *Science 278*, 82−87.
3. Hellinga, H. W. (1997) *Proc. Natl. Acad. Sci. U.S.A. 94*, 10015−10017.
4. DeGrado, W. F., Wasserman, Z. R., and Lear, J. D. (1989) *Science 243*, 622−628.
5. Hellinga, H. W. (1997) *Folding Des. 3*, R1−R8.
6. Lu, Y., and Valentine, J. S. (1997) *Curr. Opin. Struct. Biol. 7*, 495−500.
7. Regan, L. (1995) *Trends Biochem. Sci. 20*, 280−285.
8. Lippard, S. J., and Berg, J. M. (1994) *Principles of Bioinorganic Chemistry*, University Science Books, Mill Valley, CA.
9. Ibers, J. A., and Holm, R. H. (1980) *Science 209*, 223−235.
10. Stephens, P. J., Jollie, D. R., and Warshel, A. (1996) *Chem. Rev. 96*, 2491−2513.
11. Martin, J. L. (1995) *Structure 3*, 245−250.
12. Beinert, H., Holm, R. H., and Munck, E. (1997) *Science 277*, 653−659.
13. Moura, J. J. G., Goodfellow, B. J., Romao, M. J., Rusnak, F., and Moura, I. (1996) *Commun. Inorg. Chem. 19*, 47−66.
14. Holmgren, A. (1995) *Structure 3*, 239−243.
15. Hellinga, H. W., and Richards, F. M. (1991) *J. Mol. Biol. 222*, 763−785.
16. Coldren, C. D., Hellinga, H. W., and Caradonna, J. P. (1997) *Proc. Natl. Acad. Sci. U.S.A. 94*, 6635−6640.
17. Hellinga, H. W. (1998) *J. Am. Chem. Soc.* (submitted for publication).
18. Pinto, A. L., Hellinga, H. W., and Caradonna, J. P. (1997) *Proc. Natl. Acad. Sci. U.S.A. 94*, 5562−5567.
19. Wisz, M. S., Garrett, C. Z., and Hellinga, H. W. (1998) *Biochemistry* (in press).
20. Holmquist, B. (1988) *Methods Enzymol. 158*, 6−13.

21. Kunkel, T. A. (1985) *Proc. Natl. Acad. Sci. U.S.A. 82*, 448−492.
22. Hellinga, H. W., Caradonna, J. P., and Richards, F. M. (1991) *J. Mol. Biol. 222*, 787−803.
23. Katti, S. K., LeMaster, D. M., and Eklund, H. (1990) *J. Mol. Biol. 212*, 167−184.
24. Langsetmo, K., Fuchs, J. A., and Woodward, C. (1991) *Biochemistry 30*, 7603−7609.
25. Maina, C. V., Riggs, P. D., Grandea, A. G., Slatko, B. E., Moran, L. S., Tagliamonte, J. A., McReynolds, L. A., and Guam, C. (1988) *Gene 40*, 365−373.
26. Riddles, P. W., Blakely, R. L., and Zerner, B. (1983) *Methods Enzymol. 91*, 49−60.
27. Gill, S. C., and Hippel, P. H. v. (1989) *Anal. Biochem. 182*, 319−326.
28. Bradford, M. M. (1976) *Anal. Biochem. 72*, 248−254.
29. Lovenberg, W., Buchanan, B. B., and Rabinowitz, J. C. (1963) *J. Biol. Chem. 238*, 3899−3913.
30. Wertz, J. E., and Bolton, J. R. (1986) *Electron Spin Resonance: Elementary Theory and Practical Applications*, Chapman and Hall, New York.
31. Howard, J. B., and Rees, D. C. (1991) *Adv. Protein Chem. 42*, 199−280.
32. Glusker, J. P. (1991) *Adv. Protein Chem. 42*, 1−76.
33. Ponder, J. W., and Richards, F. M. (1987) *J. Mol. Biol. 193*, 775−791.
34. Eaton, W. A., and Lovenberg, W. (1973) in *Iron−Sulfur Proteins* (Lovenberg, W., Ed.) pp 131−162, Academic Press, New York.
35. Lode, E. T., and Coon, M. J. (1971) *J. Biol. Chem. 246*, 791−802.
36. Lovenberg, W., and Williams, W. M. (1969) *Biochemistry 8*, 141−148.
37. Moura, I., Huynh, B. H., Hausinger, R. P., Le Gall, J., Xavier, A. V., and Munck, E. (1980) *J. Biol. Chem. 255*, 2493−2498.
38. Bertini, I., and Luchinat, C. (1984) *Adv. Inorg. Biochem. 6*, 71−111.
39. May, S. W., and Kuo, J. Y. (1978) *Biochemistry 17*, 3333−3338.
40. Moura, I., Teixeira, M., LeGall, J., and Moura, J. J. G. (1991) *J. Inorg. Biochem. 44*, 127−139.
41. Creighton, T. E., Ed. (1989) *Protein Structure: A Practical Approach*, IRL Press at Oxford University Press, Oxford.
42. Bachmayer, H., Piette, L. H., Yasunobu, K. T., and Whiteley, H. R. (1967) *Proc. Natl. Acad. Sci. U.S.A. 57*, 122−127.
43. Mayhew, S. G., and Peel, J. L. (1966) *Biochem. J. 100*, 80−85.
44. Moura, I., Bruschi, M., Le Gall, J., Moura, J. J. G., and Xavier, A. V. (1977) *Biochem. Biophys. Res. Commun. 75*, 1037−1044.
45. Peterson, J. A., and Coon, M. J. (1968) *J. Biol. Chem. 243*, 329−334.
46. Lane, R. W., Ibers, J. A., Frankel, R. B., and Holm, R. H. (1975) *Proc. Natl. Acad. Sci. U.S.A. 72*, 2868−2872.
47. Lane, R. W., Ibers, J. A., Frankel, R. B., Papaefthymiou, G. C., and Holm, R. H. (1977) *J. Am. Chem. Soc. 99*, 84−98.
48. Archer, M., Huber, R., Tavares, P., Moura, I., Moura, J. J., Carrondo, M. A., Sieker, L. C., LeGall, J., and Ramão, M. J. (1995) *J. Mol. Biol. 251*, 690−702.
49. Holm, R. H., Kennepohl, P., and Solomon, E. I. (1996) *Chem. Rev. 96*, 2239−2314.
50. Krollis, P. J. (1991) *J. Appl. Crystallogr. 24*, 946−950.

BI980583D